Histopathology

Histopathology 2018, **72**, 270–284. DOI: 10.1111/his.13346

Aligning digital CD8$^+$ scoring and targeted next-generation sequencing with programmed death ligand 1 expression: a pragmatic approach in early-stage squamous cell lung carcinoma*

Esther Conde,[1,2,†] Alejandra Caminoa,[1,†] Carolina Dominguez,[1] Antonio Calles,[3] Stefan Walter,[4,5] Barbara Angulo,[1,2] Elena Sánchez,[1] Marta Alonso,[1] Luis Jimenez,[6] Luis Madrigal,[6] Florentino Hernando,[7] Julian Sanz-Ortega,[2,8] Beatriz Jimenez,[9] Pilar Garrido,[2,10] Luis Paz-Ares,[2,11] Javier de Castro,[2,9] Susana Hernandez[1] & Fernando Lopez-Rios[1,2]

[1]*Pathology-Laboratorio de Dianas Terapeuticas, Hospital Universitario HM Sanchinarro, Universidad CEU San Pablo, Madrid, Spain,* [2]*Centro de Investigación Biomedica en Red de Cancer (CIBERONC), Madrid, Spain,* [3]*Medical Oncology, Hospital Universitario Gregorio Marañón, Madrid, Spain,* [4]*Fundación de Investigación Sanitaria de Getafe, Madrid, Spain,* [5]*University of California San Francisco, San Francisco, CA, USA,* [6]*Thoracic Surgery, Hospital Universitario HM Sanchinarro, Madrid, Spain,* [7]*Thoracic Surgery, Hospital Clínico San Carlos, Universidad Complutense, Madrid, Spain,* [8]*Pathology, Hospital Clínico San Carlos, Universidad Complutense, Madrid, Spain,* [9]*Medical Oncology, Hospital Universitario HM Sanchinarro, Madrid, Spain,* [10]*Medical Oncology, IRYCIS, Hospital Universitario Ramón y Cajal, Universidad de Alcalá, Madrid, Spain, and* [11]*Medical Oncology, Hospital Universitario 12 de Octubre, CNIO and Universidad Complutense, Madrid, Spain*

Date of submission 20 February 2017
Accepted for publication 16 August 2017
Published online *Article Accepted* 16 August 2017

Conde E, Caminoa A, Dominguez C, Calles A, Walter S, Angulo B, Sánchez E, Alonso M, Jimenez L, Madrigal L, Hernando F, Sanz-Ortega J, Jimenez B, Garrido P, Paz-Ares L, de Castro J, Hernandez S & Lopez-Rios F (2018) *Histopathology* **72**, 270–284. https://doi.org/10.1111/his.13346

Aligning digital CD8$^+$ scoring and targeted next-generation sequencing with programmed death ligand 1 expression: a pragmatic approach in early-stage squamous cell lung carcinoma

Aims: To study programmed death ligand 1 (PD-L1) expression, tumour-infiltrating T lymphocytes (TILs) and the molecular context in patients with early-stage squamous cell lung carcinomas (SCCs).

Methods and results: The study included samples from 40 patients (discovery cohort) and 29 patients (validation cohort) diagnosed with early-stage SCC. PD-L1 immunohistochemistry (IHC) was performed with three commercially available clones (E1L3N, SP263 and SP142). CD8$^+$ TILs were scored with a digital algorithm. All tumours were analysed with targeted next-generation sequencing (NGS). Additionally, *TP53* mutations were investigated with direct sequencing. In both cohorts, we observed a significant association between CD8$^+$ TILs density and high PD-L1 IHC expression in tumour cells (TCs). Furthermore, high SP142 PD-L1 expression in immune cells (ICs) was also associated significantly with CD8$^+$ TILs density. Therefore, CD8$^+$ TILs density discriminated between patients with high versus low PD-L1 IHC expression with excellent sensitivity and specificity. Interestingly, the highest percentages of PD-L1-

Address for correspondence: F Lopez-Rios, Pathology-Laboratorio de Dianas Terapeuticas, Hospital Universitario HM Sanchinarro, C/Oña, 10, 28050 Madrid, Spain. e-mail: flopezrios@hmhospitales.com

*Presented in part at the 17th World Conference on Lung Cancer, Vienna, December 2016.

†These authors contributed equally to this paper.

positive TCs with the three antibodies were found in samples with cyclin-dependent kinase 6 (*CDK6*) amplification, with high amplification of proto-oncogene C-Myc (*CMYC*) or with cyclin D1–PI3 kinase subunit alpha (*CCND1–PIK3CA*) co-amplification. High SP142 PD-L1 IHC expression in ICs showed a non-significant correlation with *TP53* mutations. Conversely, most cases with fibroblast growth factor receptor 1 (*FGFR1*) amplification were negative for all PD-L1 clones.

Conclusions: Our preliminary results support the use of digital $CD8^+$ TILs scoring and targeted NGS alongside PD-L1 expression. The approach presented herein could help define patients with SCCs candidates to immune checkpoints inhibitors.

Keywords: CD8, next-generation sequencing, PD-L1, squamous cell lung carcinoma, TILs

Introduction

Most of the advances in the personalised treatment of non-small cell lung carcinomas (NSCLCs) have been confined to the treatment of patients with adenocarcinomas (ACs). Squamous cell carcinomas (SCCs) are addressed in lung cancer biomarker guidelines, but usually lack targetable drive alterations.[1] The arrival of immunotherapy is increasing interest into this subgroup, because of the good response to immune checkpoint inhibitors.[2] Although the importance of identifying potential immunotherapy responders accurately has never been greater, few areas in cancer biomarkers have been as contentious.[2,3] It has been proposed that the mutational or neoantigen burden, together with the density of tumour-infiltrating T lymphocytes (TILs) and the high expression of programmed death ligand 1 (PD-L1) and $CD8^+$, defines a type of tumour microenvironment predictive of response to immune checkpoint inhibitors.[2,4,5] However, these data have been challenged because some of the proposed methodologies are both difficult to reproduce in the clinical setting and are applied usually as an isolated approach and tailored to a specific design [e.g. tissue microarrays, comprehensive sequencing, complicated immunohistochemistry (IHC) scoring algorithms or gene expression profiling] (reviewed in Gibney *et al.*[2]). Therefore, it has been proposed that composite strategies might be more effective for the prediction of checkpoint inhibitors therapies.[1,2,6–9] For example, a combination of two methods [PD-L1 IHC and mRNA analysis of interferon (IFN)-γ] has been shown to improve not only the positive predictive value, but especially the negative predictive value (up to 97%) in NSCLC patients treated with durvalumab.[10,11] This situation prompted us to investigate several alternatives to the situation outlined above that are easier to reconcile with clinical practice in a series of early-stage SCCs. To our knowledge, there has not been an independent assessment of the tumour microenvironment using our strategy [i.e. ready-to-use PD-L1 IHC, automated digital $CD8^+$ TILs scoring and commercial targeted next-generation sequencing (NGS)].

Material and methods

PATIENTS AND TISSUE SAMPLES

The Institutional Ethics Committee at Grupo HM Hospitales reviewed and approved this study and regulated the need for additional specific consent. A total of 40 consecutive patients with early-stage lung SCC who underwent surgery at Hospital Universitario HM Sanchinarro from October 2008 to February 2016 were considered (discovery cohort). A previously published similar series of 29 patients from Hospital Clínico San Carlos was used as a validation cohort.[12] The material available for all tumours was formalin-fixed and paraffin-embedded (FFPE). All samples were reviewed according to the current World Health Organisation (WHO) 2015 classification by two thoracic pathologists (E.C. and A.C.). Because distinguishing SCCs from other histological types can appear extremely difficult by routine light microscopy, we used IHC as described previously[13] to ensure that only bona fide SCCs were considered (data not shown). Clinical data were retrieved from the patient medical records. Patient and tumour characteristics are summarised in Table 1.

IMMUNOHISTOCHEMISTRY

To estimate the expression of PD-L1 and the density of TILs, IHC was performed on whole FFPE freshly cut tissue sections of 4-μm thickness using an automated stainer (Benchmark ULTRA; Ventana Medical Systems, Tucson, AZ, USA) and the following primary antibodies in accordance with the manufacturer's recommendations: three anti-human PD-L1 rabbit monoclonal antibodies (clone SP263, ready to use, Ventana; clone SP142, ready to use, Ventana;

Table 1. Clinicopathological features of discovery and validation cohorts

Characteristic	Discovery cohort (n = 40)	Validation cohort (n = 29)
Sex, *n* (%)		
Male	32 (80)	26 (90)
Female	8 (20)	3 (10)
Age (years), mean (SD)	66.53 (8.99)	68.55 (10.02)
Smoking history, *n* (%)		
Former smoker	18 (46.2)	17 (60.7)
Current smoker	21 (53.8)	11 (39.3)
Unknown	1	1
Histological subtypes, *n* (%)		
Basaloid	1 (2.5)	0
Non-keratinising	18 (45)	7 (24)
Keratininising	21 (52.5)	22 (76)
Tumour size (cm), mean (SD)	3.29 (2.0)	4.30 (1.87)
Stage, *n* (%)		
IA	12 (30)	4 (14)
IB	7 (17.5)	14 (48)
IIA	6 (15)	8 (28)
IIB	6 (15)	3 (10)
IIIA	9 (22.5)	0
Relapses, *n* (%)	13 (32.5)	12 (41.4)
Deaths, *n* (%)	5 (12.5)	10 (34.5)
Relapse-free time (months), mean (SD)	23.76 (18.9)	25.77 (27.39)
Overall survival (months), mean (SD)	29.17 (19.39)	43.61 (27.41)

SD, Standard deviation.

and clone E1L3N, dilution 1:200, Cell Signaling, Danvers, MA, USA) and anti-CD8 rabbit monoclonal antibody (clone SP57, ready to use, Ventana). The OptiView Universal diaminobenzidene (DAB) IHC Detection Kit (Ventana) was used for anti-PD-L1 antibodies, whereas the anti-CD8 was visualised with the UltraView Universal DAB IHC Detection Kit (Ventana). Sections were counterstained with haematoxylin. For optimisation of the PD-L1 staining, a PD-L1-positive SCC was included in all the slides as an external positive control and alveolar macrophages were also considered as internal positive controls. The lung non-neoplastic parenchyma in each case was used as a negative control. For the TILs expression, on-slide human tonsil was used as a positive control.

INTERPRETATION OF PD-L1 IHC EXPRESSION

Immunostains were evaluated independently by two pathologists (E.C. and A.C.) blinded to the clinical and pathological data. When a discrepancy was observed, a consensus was reached for the final score. Regarding PD-L1 IHC, the percentage of tumour cells (TCs) and tumour-infiltrating immune cells (ICs) with positive membranous ± cytoplasmic staining of any intensity was assessed and dichotomised as positive or negative for the 1, 5, 10, 25 and 50% cut-offs, according to the criteria used in the corresponding clinical trials.[14] We defined heterogeneity as the variance in staining between fields of view within a given section, as described previously.[15] Furthermore, we considered two different patterns: 'geographic heterogeneity' (heterogeneity at ×40 magnification) and 'mosaic heterogeneity' (heterogeneity at ×200 magnification).

AUTOMATED DIGITAL SCORING OF CD8$^+$ TILS

Sections stained for CD8 were scanned digitally (iScan Coreo; Ventana) with a × 20 objective (0.46 μm/pixel). The whole-section images were visualised using Ventana Virtuoso software (Ventana) and one field of view from each of the three compartments were outlined at ×200 magnification: intra-epithelial, peritumoral stroma and intratumoral stroma, as described previously.[16,17] Subsequently, all selected areas were scored automatically using an off-label nuclear algorithm on the Ventana Virtuoso software (Ventana) (Figure 1). The density of CD8$^+$ cells, calculated by dividing the number of positive cells by the size of the region (cells/mm^2), was recorded with the same approach used by other authors.[18]

MOLECULAR ANALYSIS

We performed a targeted NGS panel (Oncomine™ Focus Assay; ThermoFisher Scientific, Fremont, CA, USA) for screening of mutations, copy number variations (CNVs) and fusions in 52 genes, using the Ion Torrent PGM™ platform (ThermoFisher Scientific) (see Supporting information). Based on a previous

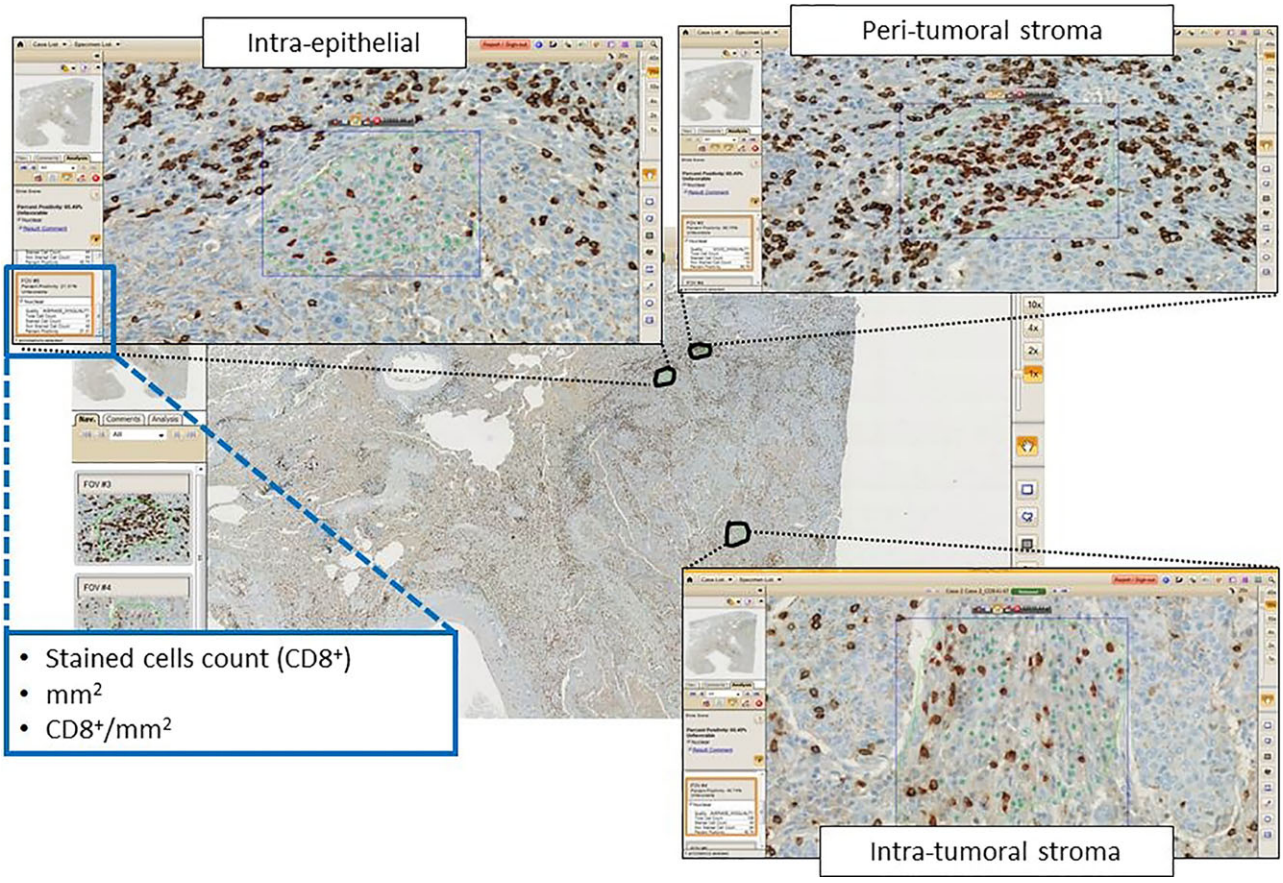

Figure 1. Digital scoring of $CD8^+$ tumour-infiltrating T lymphocyte (TIL) in three compartments.

report[19] linking specific mutations with neoepitope load, we also investigated *TP53* by direct sequencing (see Supporting information).

STATISTICAL ANALYSIS

We evaluated the association between PD-L1 expression and clinicopathological features, $CD8^+$ TILs and molecular alterations along with disease-free survival (DFS) and overall survival (OS). The concordance between the PD-L1 IHC clones was determined with Pearson's correlation coefficient (ρ). To assess concordance of scores between pathologists, intraclass correlation coefficients (ICCs) and Fleiss ϰ coefficient were calculated for each antibody. ICCs of 0.85 or higher and a ϰ coefficient of 0.8 or higher indicate almost perfect agreement, as described previously.[20] Frequencies were compared using Fisher's exact test. For comparison of continuous variables across PD-L1 expression thresholds, analysis of variance (ANOVA) was used. Receiver operating characteristic (ROC) curves were used to compare different marker cut-offs for $CD8^+$ T cell density that correlated with high PD-L1 expression by different assays and in different tumoral compartments. Optimal cut-points were defined as maximising the sum of sensitivity and specificity of $CD8^+$ T cell density as predictive markers of high PD-L1 expression. Survival analysis was performed using the Kaplan–Meier method via the log-rank test. All analyses were performed in R version 3.2.3 (R Core Team, Vienna, Austria), were two-sided, and *P*-values < 0.05 indicated statistical significance.

Results

PD-L1 IHC EXPRESSION

PD-L1 IHC expression with the three antibodies evaluated on TCs and ICs according to the different criteria used in clinical trials are presented in Table 2, and a representative example is illustrated in Figure 2. In the discovery cohort, all positive tumours showed a spatial heterogenous staining pattern on

Table 2. PD-L1 IHC expression in TCs and ICs using different cut-offs* on discovery and validation cohorts

	PD-L1 IHC expression in TCs								PD-L1 IHC expression in ICs					
	1%		5%		25%		50%		1%		5%		10%	
Clones	Negative *n* (%)	Positive *n* (%)	Negative *n* (%)	Positive *n* (%)	Negative *n* (%)	Positive *n* (%)	Negative *n* (%)	Positive *n* (%)	Negative *n* (%)	Positive *n* (%)	Negative *n* (%)	Positive *n* (%)	Negative *n* (%)	Positive *n* (%)
	Discovery cohort (*n* = 40)													
E1L3N	21 (52.5)	19 (47.5)	29 (72.5)	11 (27.5)	34 (85)	6 (15)	35 (87.5)	5 (12.5)	9 (22.5)	31 (77.5)	22 (55)	18 (45)	28 (70)	12 (30)
SP263	16 (40)	24 (60)	24 (60)	16 (40)	30 (75)	10 (25)	35 (87.5)	5 (12.5)	3 (7.5)	37 (92.5)	11 (27.5)	29 (72.5)	19 (47.5)	21 (52.5)
SP142	27 (67.5)	13 (32.5)	34 (85)	6 (15)	35 (87.5)	5 (12.5)	36 (90)	4 (10)	3 (7.5)	37 (92.5)	12 (30)	28 (70)	23 (57.5)	17 (42.5)
	Validation cohort (*n* = 29)													
E1L3N	12 (41.4)	17 (58.6)	19 (65.5)	10 (34.5)	22 (75.9)	7 (24.1)	24 (82.8)	5 (17.2)	5 (17.2)	24 (82.8)	21 (72.4)	8 (27.6)	25 (86.2)	4 (13.8)
SP263	7 (24.1)	22 (75.9)	13 (44.8)	16 (55.2)	21 (72.4)	8 (27.6)	24 (82.8)	5 (17.2)	1 (3.4)	28 (96.6)	12 (41.4)	17 (58.6)	16 (55.2)	13 (44.8)
SP142	16 (55.2)	13 (44.8)	21 (72.4)	8 (27.6)	26 (89.7)	3 (10.3)	26 (89.7)	3 (10.3)	1 (3.4)	28 (96.6)	17 (58.6)	12 (41.4)	26 (89.7)	3 (10.3)

ICs, Immune cells; IHC, Immunohistochemistry; TCs, Tumour cells; PD-L1, Programmed death ligand 1; IHC, Immunohistochemistry.
*Negative includes values < to the cut-off; positive includes values ≥ to the cut-off.

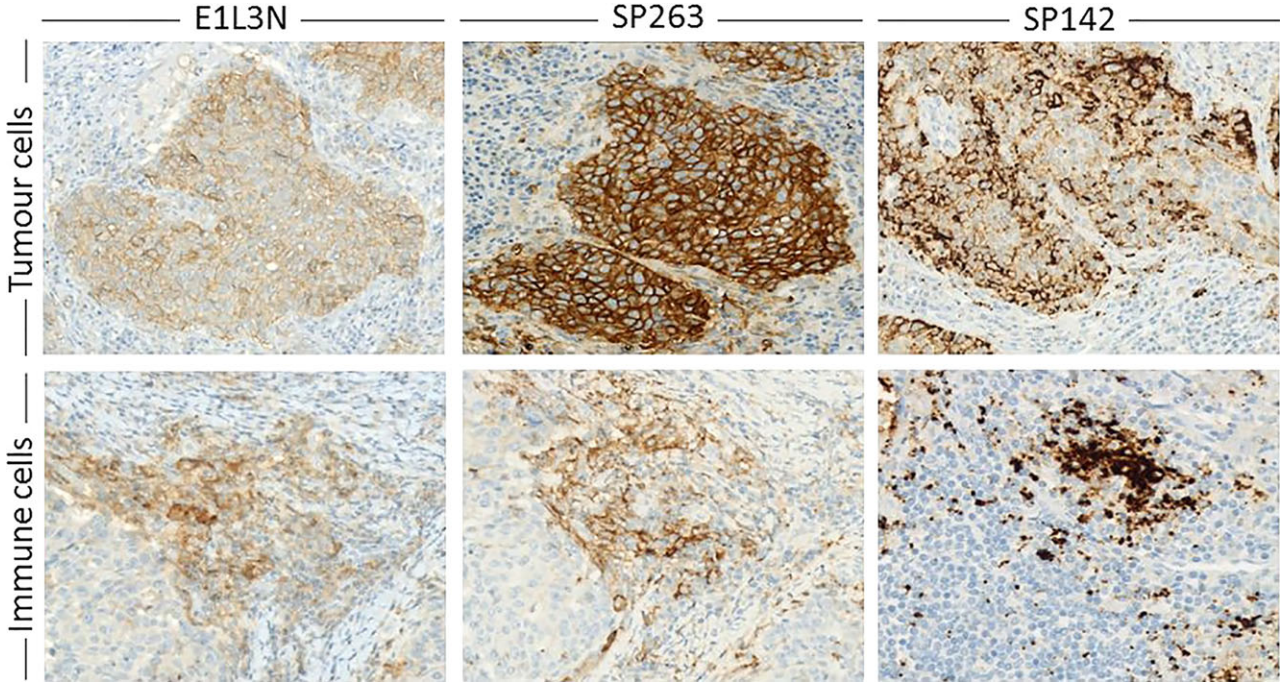

Figure 2. Representative images of high programmed death ligand 1 (PD-L1) expression in tumour cells and immune cells.

TCs with the three clones, which was geographic in 21% and mosaic in 79% of the cases. The results were almost identical in the validation cohort: 23 and 77%, respectively. The concordance between pathologists' scores for TCs and ICs was almost perfect in both cohorts. In the discovery cohort, for TCs the ICCs were 0.93 [95% confidence interval (CI): 0.88–0.96], 0.96 (95% CI: 0.93–0.98) and 0.99 (95% CI: 0.97–0.99) for E1L3N, SP263 and SP142, respectively; and for ICs, 0.92 (95% CI: 0.86–0.96), 0.92 (95% CI: 0.86–0.96) and 0.96 (95% CI: 0.92–0.98) for E1L3N, SP263 and SP142, respectively. In the validation cohort, for TCs the ICCs were 0.96 (95% CI: 0.92–0.98), 0.97 (95% CI: 0.92–0.98) and 0.97 (95% CI: 0.93–0.98) for E1L3N, SP263 and SP142, respectively; and for ICs, the concordance was not as good with values of 0.77 (95% CI: 0.57–0.88), 0.81 (95% CI: 0.63–0.91) and 0.76 (95% CI: 0.55–0.88) for E1L3N, SP263 and SP142, respectively. Considering the highest cut-off in TCs (≥ 50%), the interobserver concordance was excellent, with exactly the same values in both series (i.e. $\varkappa$ coefficient of 0.87 for E1L3N and 1 for SP263 and SP142). In both cohorts, there was a very good correlation between the E1L3N and the SP263 clones ($\rho = 0.94$ in the discovery set and $\rho = 0.99$ in the validation cohort), while a lower correlation was observed between the SP263 and SP142 antibodies ($\rho = 0.88$ in the discovery cohort versus $\rho = 0.87$ in the validation cohort). Interestingly, we noted a perfect agreement between the E1L3N and SP263 clones using the 50% cut-off in both cohorts. Unsurprisingly, the correlation between the antibodies was worse when considering ICs (discovery cohort: $\rho = 0.88$ between E1L3N and SP263 and $\rho = 0.74$ between E1L3N and SP142 and SP263 and SP142; validation cohort: $\rho = 0.86$ between E1L3N and SP263, $\rho = 0.70$ between E1L3N and SP142 and $\rho = 0.68$ between SP263 and SP142).

CORRELATION OF PD-L1 IHC EXPRESSION WITH CLINICOPATHOLOGICAL CHARACTERISTICS

PD-L1 IHC expression in TCs with the three antibodies was higher in current smokers than in former smokers (discovery cohort, mean: 16.19 versus 3.11; $P = 0.048$ for E1L3N clone; mean: 22.57 versus 7.28; $P = 0.064$ for SP263 clone; and mean: 12.62 versus 0.33; $P = 0.026$ for SP142 clone). There was a similar trend in the validation cohort, but the results were not significant (data not shown). There were no other relevant associations.

CORRELATION OF PD-L1 IHC EXPRESSION WITH $CD8^+$ TILS

We found that SCCs exhibited different topographic $CD8^+$ TILs densities (peritumoral stroma, intratumoral

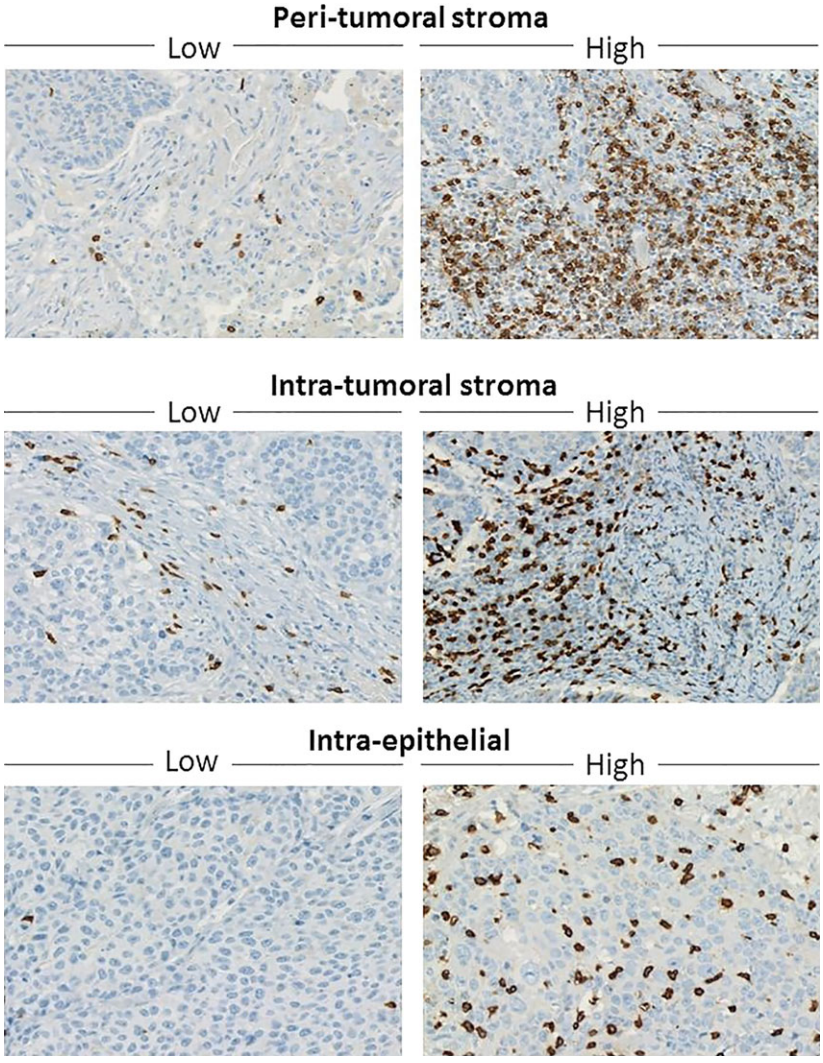

Figure 3. Representative images of low and high $CD8^+$ tumour-infiltrating T lymphocyte (TIL) density within the three compartments.

stroma and intra-epithelial). In the discovery cohort, $CD8^+/mm^2$ TILs within the peritumoral stromal compartment ranged from 312 to 4793 [mean ± standard deviation (SD): 1807.6 ± 933.64]; within the intratumoral stromal region ranged from 120 to 3624 (mean ± SD: 1253.6 ± 830.19); and within the intra-epithelial compartment ranged from 17 to 2002 (mean ± SD: 242.22 ± 333.01). Representative images are shown in Figure 3. In the validation cohort, the results were strikingly similar in the intra-epithelial compartment. $CD8^+/mm^2$ TILs within the peritumoral stromal compartment ranged from 91 to 2721 (mean ± SD: 1070.31 ± 687.43); within the intratumoral stromal region ranged from 20 to 3023 (mean ± SD: 1061.62 ± 768.78); and within the intra-epithelial compartment ranged from eight to 2133 (mean ± SD: 243.55 ± 406.50). In the discovery cohort, we observed a significant association between both the intra-epithelial and the peritumoral stromal $CD8^+$ TILs density and high (≥ 50%) PD-L1 IHC expression in TCs with the three clones (Table 3). The intra-epithelial finding was replicated consistently in the validation cohort, but the peritumoral compartment data were observed only with the SP142 clone. Furthermore, high (≥ 10%) SP142 PD-L1 expression in ICs was associated significantly with intra-epithelial $CD8^+$ TILs density in the discovery cohort and with peritumoral and intratumoral $CD8^+$ TILs densities in the validation cohort (Table 3).

In addition, ROC analyses were used to determine the optimal cut-off value for $CD8^+$ TILs density that discriminates between patients with high versus low PD-L1 IHC expression. As illustrated in Figure 4A,B, the presence of 416 $CD8^+/mm^2$ within the intra-epithelial compartment had 94% specificity and 80%

Table 3. Analysis of variance (ANOVA) between PD-L1 IHC expression in TCs and ICs using the highest cut-off and automatically scored $CD8^+$ TILs on discovery and validation cohorts

	PD-L1 IHC expression in TCs									PD-L1 IHC expression in ICs		
	E1L3N			SP263			SP142			SP142		
$CD8^+$ TILs density (mean)	Negative (< 50%)	Positive (≥ 50%)	*P*	Negative (< 50%)	Positive (≥ 50%)	*P*	Negative (< 50%)	Positive (≥ 50%)	*P*	Negative (< 10%)	Positive (≥ 10%)	*P*
	Discovery cohort (*n* = 40)											
Total	35	5		35	5		36	4		23	17	
Peri-tumoral stroma	1689.94	2631.20	**0.033**	1689.94	2631.20	**0.033**	1677.25	2980.75	**0.006**	1716.09	1931.41	0.478
Intra-tumoral stroma	1246.29	1304.80	0.885	1246.29	1304.80	0.885	1241.17	1365.5	0.780	1095.74	1467.18	0.165
Intra-epithelial	171.06	740.40	**< 0.001**	171.06	740.40	**< 0.001**	180.94	793.75	**< 0.001**	141.74	378.18	**0.024**
	Validation cohort (*n* = 29)											
Total	24	5		24	5		26	3		26	3	
Peri-tumoral stroma	1029.12	1268.00	0.489	1029.12	1268.00	0.489	980.35	1850.00	**0.035**	972.35	1919.33	**0.021**
Intra-tumoral stroma	1105.04	853.20	0.515	1105.04	853.20	0.515	1044.77	1207.67	0.735	941.65	2101.33	**0.011**
Intra-epithelial	167.21	610.00	**0.024**	167.21	610.00	**0.024**	162.92	942.33	**< 0.001**	220 00	447.33	0.369

ICs, Immune cells; IHC, Immunohistochemistry; TCs, Tumour cells; TILs, Tumour-infiltrating lymphocytes; PD-L1, Programmed death ligand 1. Significant *P*-values are shown in bold type.

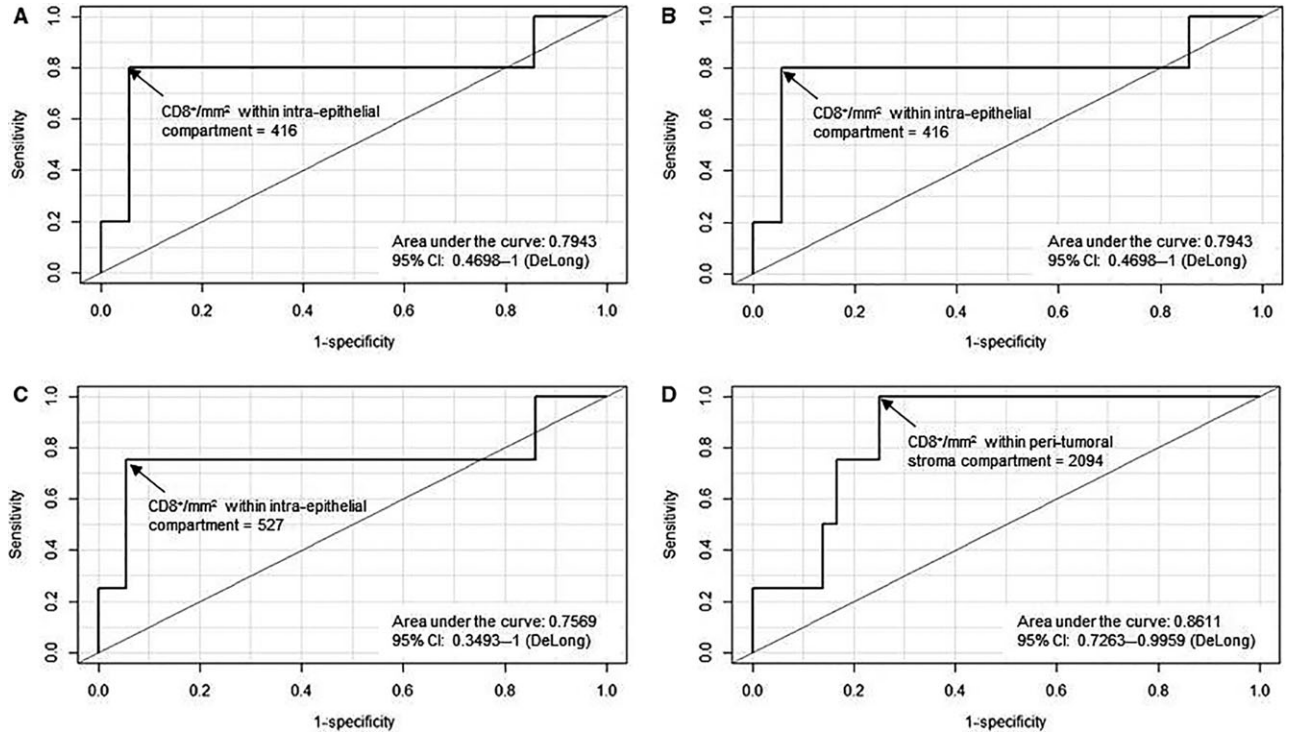

Figure 4. ROC curves analyses identified 416 $CD8^+/mm^2$ or 527 $CD8^+/mm^2$ in the intra-epithelial compartment as the optimal cut-off values for identifying patients with high (≥50%) programmed death ligand 1 (PD-L1) expression with clones E1L3N/SP263 (**A**,**B**) or clone SP142 (**C**), respectively. In addition, 2094 $CD8^+$ TIL density in the peri-tumoral stromal compartment was required to discriminate between high versus low SP142 PD-L1 expression in tumour cells (TCs) (**D**). Data from the discovery cohort.

sensitivity for identifying patients with high (≥ 50%) E1L3N and SP263 PD-L1 expression in TCs. Regarding SP142 PD-L1 expression, a density of 527 $CD8^+/mm^2$ within the intra-epithelial compartment had a 94% specificity and 75% sensitivity (Figure 4C), whereas in the peritumoral stromal compartment, 2094 $CD8^+/mm^2$ was required for a 75% specificity and 100% sensitivity (Figure 4D). Using the above cut-off values, in the validation cohort the results were as follows. The presence of 416 $CD8^+/mm^2$ within the intra-epithelial compartment had 88% specificity and 40% sensitivity for identifying patients with high (≥ 50%) E1L3N and SP263 PD-L1 expression in TCs. Regarding SP142 PD-L1 expression, a density of 527 $CD8^+/mm^2$ within the intra-epithelial compartment had 92% specificity and 67% sensitivity, whereas in the peritumoral stromal compartment the specificity and sensitivity were 33 and 92%, respectively.

CORRELATION OF PD-L1 IHC EXPRESSION WITH MOLECULAR ALTERATIONS

Molecular alterations found in both cohorts are summarised in Table 4. In the discovery cohort, five of 26 (19.2%) patients with molecular alterations exhibited both mutations and CNVs. Five of 10 (50%) tumours with CNVs showed copy number gains in more than one gene (data not shown). *TP53* mutations were concurrent with PI3 kinase subunit alpha (*PIK3CA*) mutations in all four positive cases and with fibroblast growth factor receptor 1 (*FGFR1*), cyclin-dependent kinase 6 (*CDK6*), *PIK3CA*, proto-oncogene C-Myc (*CMYC*) or Erb-B2 receptor tyrosine kinase 2 (*ERBB2*) amplifications in one patient. In the validation cohort, six of 20 (30%) patients with molecular alterations showed both mutations and CNVs and three of nine (33.3%) tumours with CNVs exhibited gains in more than one gene (data not shown). *TP53* mutations were also concurrent with *PIK3CA* mutations in two cases, with epidermal growth factor receptor (*EGFR*), cyclin D1 (*CCND1*), *FGFR1* or *ERBB2* amplifications in two patients and with *PIK3CA* or *CMYC* amplifications in one patient.

In the discovery cohort, comparative analyses revealed that only high (≥ 10%) SP142 PD-L1 IHC expression in ICs showed a non-significant correlation with *TP53* mutations ($P = 0.099$). Interestingly, the highest percentages of PD-L1-positive TCs with the

Table 4. Correlation between PD-L1 IHC expression in TCs and ICs using the highest cutoff and molecular alterations on discovery and validation cohorts

Molecular alterations, *n* (%)	Total	PD-L1 IHC expression in TCs									PD-L1 IHC expression in ICs		
		E1L3N			SP263			SP142			SP142		
		Negative (< 50%)	Positive (≥ 50%)	*P*	Negative (< 50%)	Positive (≥ 50%)	*P*	Negative (< 50%)	Positive (≥ 50%)	*P*	Negative (< 10%)	Positive (≥ 10%)	*P*
		Discovery cohort											
Total	40	35	5		35	5		36	4		23	17	
Mutations													
*TP53**	19 (51.4)	15 (78.9)	4 (21.1)	0.340	15 (78.9)	4 (21.1)	0.340	16 (84.2)	3 (15.8)	0.604	8 (42.1)	11 (57.9)	0.099
PIK3CA	4 (10)	3 (75)	1 (25)	0.427	3 (75)	1 (25)	0.427	3 (75)	1 (25)	0.355	1 (25)	3 (75)	0.294
FGFR3	1 (2.5)	1 (100)	0	1.000	1 (100)	0	1.000	1 (100)	0	1.000	1 (100)	0	1.000
KIT	1 (2.5)	1 (100)	0	1.000	1 (100)	0	1.000	1 (100)	0	1.000	1 (100)	0	1.000
Copy number gains													
CDK6	1 (2.5)	0	1 (100)	0.125	0	1 (100)	0.125	0 (0)	1 (100)	0.100	1 (100)	0	1.000
CCND1	4 (10)	4 (100)	0	1.000	4 (100)	0	1.000	4 (100)	0 (0)	1.000	2 (50)	2 (50)	1.000
PIK3CA	4 (10)	3 (75)	1 (25)	0.427	3 (75)	1 (25)	0.427	3 (75)	1 (25)	0.355	1 (25)	3 (75)	0.294
FGFR1	4 (10)	4 (100)	0	1.000	4 (100)	0	1.000	4 (100)	0 (0)	1.000	3 (75)	1 (25)	0.624
EGFR	1 (2.5)	1 (100)	0	1.000	1 (100)	0	1.000	1 (100)	0	1.000	0	1 (100)	0.425
CMYC	2 (5)	1 (50)	1 (50)	0.237	1 (50)	1 (50)	0.237	1 (50)	1 (50)	0.192	1 (50)	1 (50)	1.000
NMYC	1 (2.5)	1 (100)	0	1.000	1 (100)	0	1.000	1 (100)	0	1.000	1 (100)	0	1.000
ERBB2	1 (2.5)	1 (100)	0	1.000	1 (100)	0	1.000	1 (100)	0	1.000	0	1 (100)	0.425
		Validation cohort											
Total	29	24	5		24	5		26	3		26	3	
Mutations													
*TP53**	16 (61.5)	14 (87.5)	2 (12.5)	0.340	14 (87.5)	2 (12.5)	0.340	14 (87.5)	2 (12.5)	1.000	14 (87.5)	2 (12.5)	1.000
PIK3CA	3 (10.3)	2 (66.7)	1 (33.3)	0.446	2 (66.7)	1 (33.3)	0.446	3 (100)	0	1.000	3 (100)	0	1.000
Copy number gains													
CCND1	2 (6.9)	1 (50)	1 (50)	0.320	1 (50)	1 (50)	0.320	1 (50)	1 (50)	0.200	2 (100)	0	1.000

Table 4. *(Continued)*

Molecular alterations, *n* (%)	Total	PD-L1 IHC expression in TCs								PD-L1 IHC expression in ICs		
		E1L3N			SP263			SP142		SP142		
		Negative (< 50%)	Positive (≥ 50%)	*P*	Negative (< 50%)	Positive (≥ 50%)	*P*	Negative (< 50%)	Positive (≥ 50%)	*P*	Negative (< 10%)	Positive (≥ 10%)	*P*
PIK3CA	1 (3.4)	0	1 (100)	0.172	0	1 (100)	0.172	0	1 (100)	0.103	1 (100)	0	1.000
FGFR1	3 (10.3)	2 (66.7)	1 (33.3)	0.446	2 (66.7)	1 (33.3)	0.446	2 (66.7)	1 (33.3)	0.288	3 (100)	0	1.000
EGFR	4 (13.8)	4 (100)	0	1.000	4 (100)	0	1.000	4 (100)	0	1.000	4 (100)	0	1.000
CMYC	1 (3.4)	1 (100)	0	1.000	1 (100)	0	1.000	1 (100)	0	1.000	1 (100)	0	1.000
ERBB2	2 (6.9)	2 (100)	0	1.000	2 (100)	0	1.000	2 (100)	0	1.000	2 (100)	0	1.000

*Data not available for three cases in both cohorts.

three antibodies were found in samples with *CDK6* amplification (range: 60–90%) or with high amplification of *CMYC* (range: 60–80%). Conversely, cases with *FGFR1* amplification were negative for all PD-L1 clones. In the validation cohort, *CDK6* amplifications were not identified and the only case of high *CMYC* amplification was negative. One of two *FGFR1*-amplified cases was PD-L1-positive in TCs. The highest percentages of PD-L1-positive TCs with the three antibodies were found in one of the samples with *CCND1* and *PIK3CA* co-amplification.

PROGNOSTIC SIGNIFICANCE OF PD-L1 IHC EXPRESSION AND CD8$^+$ TILS

In the discovery cohort, there were no significant differences in OS or DFS according to PD-L1, although high (≥ 50%) PD-L1 IHC expression in TCs assessed with the three antibodies showed a non-significant trend for better DFS (log-rank $P = 0.103$ for E1L3N and SP263, log-rank $P = 0.173$ for SP142). Regarding CD8$^+$ TILs and using the mean value as cut-off, high intra-epithelial (≥ 242) CD8$^+$ density was associated marginally with improved OS (log-rank $P = 0.059$) (Figure 5A), but was related significantly to DFS (log-rank $P = 0.026$) (Figure 5B). High peritumoral stroma and intratumoral stroma CD8$^+$ densities were not associated with improved OS (log-rank $P = 0.940$ and 0.301, respectively) or DFS (log-rank $P = 0.396$ and 0.447, respectively). Survival differences were not observed in the validation cohort, due probably to the small sample size.

Discussion

In this study, we wanted to align PD-L1 IHC with the evaluation of TILs and the genomic annotation of early-stage SCCs for three main reasons. First, the lack of interclone, interlaboratory and interobserver uniformity in assay performance and assay interpretation, together with the frequent occurrence of heterogeneous expression, may preclude the use of PD-L1 IHC as a final predictive test for immune checkpoint inhibitors.[2,21–28] Although most published series, including the present study, show a reasonable concordance between the different PD-L1 clones, there are some differences.[29–33] Along these lines, it is worth emphasising that the PD-L1 expression levels have been correlated with response to anti-PD-1 or anti PD-L1 agents.[34,35] Furthermore, due to heterogeneous expression, sensitivity in small biopsies has been challenged.[36] It has been proposed that staining

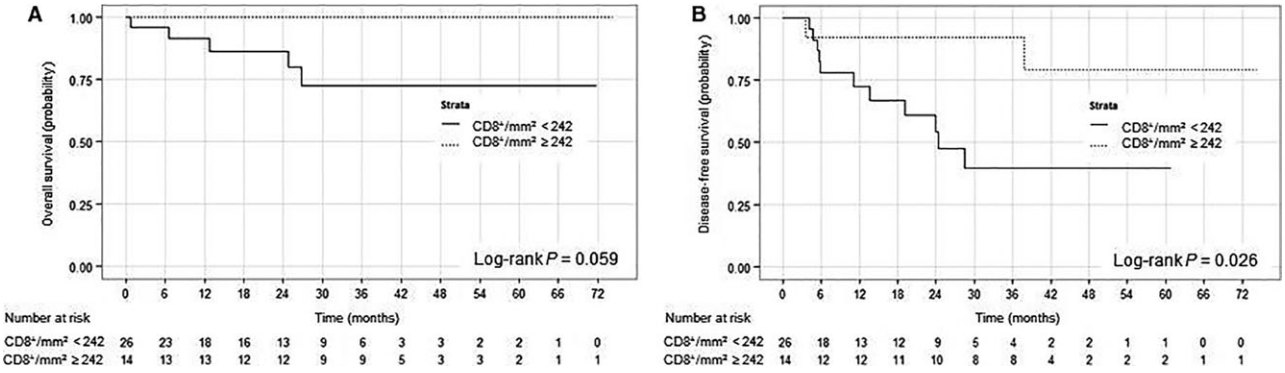

Figure 5. Kaplan–Meier curves showing overall survival (OS) (**A**) and disease-free survival (DFS) (**B**) of patients with high and low intra-epithelial $CD8^+$ T tumour-infiltrating T lymphocyte (TIL) density. The *P*-values were calculated using the log-rank test.

of more than six fragments in small biopsies or one block in surgical specimens[15,37] is needed to avoid underestimating the PD-L1 status. Unexpectedly, heterogeneity of PD-L1 expression was always present in our series. Considering (i) the reasons stated above, (ii) the small size and limited number of fragments of most lung biopsies and (iii) the lack of standardisation of the pre-analytical variables that can yield a false-negative result in a number of cases,[38] it is probably wise to state that negative PD-L1 expression alone is not enough to exclude patients from treatment.[3] Therefore, a multiparametric model combining other biomarkers might best predict response to checkpoint inhibitors (see below).

Secondly, although in NSCLCs TILs scoring is becoming an established prognostic parameter[39–47] and PD-L1 expression is associated clearly with TILs,[47–52] combining both markers in real clinical practice has remained elusive. In our opinion, the main reasons are the lack of standardisation of the assessment tools and the limited enthusiasm for retesting correlations or methodologies established by others (see below). Due to a series of factors which often coexist (i.e. use of tissue microarrays, manual scoring or scarcely available commercial algorithms), it is difficult to apply the findings published in the literature to the clinical reality.[16,18,37,45,49,51,53] For example, in a recent review of studies that focused on the assessment of TILs in NSCLCs, only 20% of them used whole sections and digital cut-offs for this purpose.[42] We showed that abundant $CD8^+$ TILs were associated with high PD-L1 expression in TCs. Of all three compartments, the intra-epithelial infiltration correlated most clearly with PD-L1 expression, consistent with a recent report in lung ACs.[49] Therefore, this approach could be extrapolated to small biopsies, in which the amount of stroma is usually extremely scarce. In contradistinction with lung ACs (E. Conde, unpublished data), the overall solid pattern of growth of lung SCCs allowed for a somewhat easy separation of the three compartments with the image analysis software. Other authors have attempted successfully to use image analysers to quantitate $CD8^+$ TILs,[18,37,54] including the use of modified nuclear algorithms,[50,55,56] but we believe that our experience with the digital methodology reported herein is unique. Although the main limitation of our study is that these small cohorts were not treated with checkpoint inhibitors, the perfect replication of the intra-epithelial data validates further the validity of our results. To partially overcome the aforementioned shortcomings, we used whole-tissue sections and commercially available tools, so our findings could be replicated and validated elsewhere. As has been suggested, we believe that this approach (i.e. use of digital pathology and image analysis software on whole slides) could overcome the alleged lack of inter- and intra-observer reproducibility for both quantifying and localising TILs.[16,40,56] In agreement with other authors, higher $CD8^+$ TILs were associated with a better prognosis in SCCs.[37,39,46,50] Similarly, we observed a trend towards a better outcome in PD-L1-positive patients with SCCs.[37,46,47,50,57–61] Interestingly, in some of these latter series the survival benefit of PD-L1 expression (including ICs) or higher CD8 + TILs are lost or even reversed when only ACs or non-SCC are considered.[46,57–59,61] Nevertheless, the prognostic value of PD-L1 expression in NSCLCs is still under debate.[48,49,51,59,62–64]

Thirdly, because (i) a synergistic therapeutic effect has been proposed for the combination of some targeted therapies and immune checkpoints inhibitors,[62] and (ii) 'broad molecular profiling' or 'multiplexed genetic sequencing panels' are being recommended in international guidelines,[65,66] we hypothesised that an off-the-shelf targeted resequencing assay could help to

predict the status of PD-L1 in SCCs. Although this strategy has been challenged in a small series of SCCs ($n = 6$),[67] several lines of evidence have highlighted the selective immune properties of individual (or limited) genomic alterations in NSCLCs.[9,68–70] In addition, a recent report has determined the immunogenicity of some specific missense mutations in SCCs,[19] so we have also investigated one not included in the commercial panel (*TP53*). Overall, an expected variety of genomic alterations in SCCs were found in our study.[19,60,71–75] Findings should be interpreted with caution to avoid sample size bias (i.e. both cohorts are small and the number of patients with specific molecular alterations is limited), but they are consistent with previous observations (see below). Interestingly, SP142 PD-L1 IHC expression in ICs showed a non-significant trend with *TP53* mutations. A very similar association has been described recently in surgically resected ACs studied with p53 IHC as a surrogate marker of the p53 status.[76] Accordingly, it has been proposed that scoring of PD-L1 ICs may increase the accuracy of PD-L1 expression.[9] In agreement with our results, high copy number levels of *MYC* have been shown to induce PD-L1 expression in several tumour types,[77] but there is no positive correlation between *FGFR1* amplification and PD-L1 expression in lung SCCs.[78] Remarkably, our finding concerning the highest percentages of PD-L1-positive TCs being found in the patient with *CDK6* amplification replicates gene expression profiling data, in which up-regulation of *PD-L1* and *CDK6* overlapped perfectly in the same group of SCCs.[79]

In conclusion, if we assume that PD-L1 IHC inter-observer agreement might be more challenging than the concordance between assays (or laboratories, for that matter),[23,60] the methodologies presented herein could help refine SCC specimens with lower percentages of PD-L1-positive cells, or even those completely negative. The increasing popularity of digital pathology and targeted NGS could provide an opportunity to improve current biomarker algorithms through multiparametric selection of patients' candidates to immune checkpoint inhibitors.

Acknowledgements

F.L.-R. acknowledges his gratitude to R. Franklin for her contribution to this work. The help of the Tumour Bank at Hospital Universitario HM Sanchinarro and the BioBank of IdISSC at Hospital Clínico San Carlos (B.0000725) is also gratefully acknowledged. This study was funded partially by Instituto de Salud Carlos III (ISCIII), Fondos FEDER-Plan Estatal de I+D+I 2013-2016 (PI14-01176, PIE15/00076, PI14/01964) and Roche Spain.

Conflict of Interests

Regarding the scope of this work, F.L.-R. has received honoraria from Roche and Life Technologies. The remaining authors declare no conflicts of interest.

References

1. Bernicker E. Biomarker testing in non-small cell lung cancer: a clinician's perspective. *Arch. Pathol. Lab. Med.* 2015; **139**; 448–450.
2. Gibney GT, Weiner LM, Atkins MB. Predictive biomarkers for checkpoint inhibitor-based immunotherapy. *Lancet Oncol.* 2016; **17**; e542–e551.
3. Sacher AG, Gandhi L. Biomarkers for the clinical use of PD-1/PD-L1 inhibitors in non-small-cell lung cancer: a review. *JAMA Oncol.* 2016; **2**; 1217–1222.
4. Ock CY, Keam B, Kim S *et al.* Pan-cancer immunogenomic perspective on the tumor microenvironment based on PD-L1 and CD8 T-cell infiltration. *Clin. Cancer Res.* 2016; **22**; 2261–2270.
5. Teng MW, Ngiow SF, Ribas A, Smyth MJ. Classifying cancers based on T cell infiltration and PD-L1. *Cancer Res.* 2015; **75**; 2139–2145.
6. Bhaijee F, Anders RA. PD-L1 expression as a predictive biomarker: is absence of proof the same as proof of absence? *JAMA Oncol.* 2016; **2**; 54–55.
7. Hansen AR, Siu LL. PD-L1 testing in cancer: challenges in companion diagnostic development. *JAMA Oncol.* 2016; **2**; 15–16.
8. Miller RA, Miller TN, Cagle PT. PD-1/PD-L1, only a piece of the puzzle. *Arch. Pathol. Lab. Med.* 2016; **40**; 1187–1188.
9. Lizotte PH, Ivanova EV, Awad MM *et al.* Multiparametric profiling of non-small-cell lung cancers reveals distinct immunophenotypes. *JCI Insight* 2016; **1**; e89014.
10. Higgs BW, Morehouse C, Streicher K *et al.* Relationship of baseline tumoral IFNγ mRNA and PD-L1 protein expression to overall survival in durvalumab-treated NSCLC patients. *J. Clin. Oncol* 2016; **34** (Suppl 15); 3036–3036.
11. Higgs BW, Robbins PB, Blake-Haskins JA *et al.* High tumoral IFNγ mRNA, PD-L1 protein, and combined IFNγ mRNA/PD-L1 protein expression associates with response to durvalumab (anti-PD-L1) monotherapy in NSCLC patients. European Cancer Congress 2015; Vienna; 25–29 September. Abstract 15LBA.
12. Hernández-Prieto S, Romera A, Ferrer M *et al.* A 50-gene signature is a novel scoring system for tumor-infiltrating immune cells with strong correlation with clinical outcome of stage I/II non-small cell lung cancer. *Clin. Transl. Oncol.* 2015; **17**; 330–338.
13. Conde E, Angulo B, Redondo P *et al.* The use of P63 immunohistochemistry for the identification of squamous cell carcinoma of the lung. *PLoS ONE* 2010; **5**; e12209.
14. Hirsch FR, Scagliotti GV, Mulshine JL *et al.* Lung cancer: current therapies and new targeted treatments. *Lancet* 2017; **389**; 299–311.
15. Rehman JA, Han G, Carvajal-Hausdorf DE *et al.* Quantitative and pathologist-read comparison of the heterogeneity of

programmed death-ligand 1 (PD-L1) expression in non-small cell lung cancer. *Mod. Pathol.* 2016; **30**; 340–349.
16. Donnem T, Hald SM, Paulsen EE *et al.* Stromal CD8+ T-cell density – a promising supplement to TNM staging in non-small cell lung cancer. *Clin. Cancer Res.* 2015; **21**; 2635–2643.
17. Salgado R, Denkert C, Demaria S *et al.* The evaluation of tumor-infiltrating lymphocytes (TILs) in breast cancer: recommendations by an International TILs Working Group 2014. *Ann. Oncol.* 2015; **26**; 259–271.
18. Gainor JF, Shaw AT, Sequist LV *et al.* EGFR mutations and ALK rearrangements are associated with low response rates to PD-1 pathway blockade in non-small cell lung cancer: a retrospective analysis. *Clin. Cancer Res.* 2016; **22**; 4585–4593.
19. Campbell JD, Alexandrov A, Kim J *et al.* Distinct patterns of somatic genome alterations in lung adenocarcinomas and squamous cell carcinomas. *Nat. Genet.* 2016; **48**; 607–616.
20. Rimm DL, Han G, Taube JM *et al.* A prospective, multi-institutional, pathologist-based assessment of 4 immunohistochemistry assays for PD-L1 expression in non-small cell lung cancer. *JAMA Oncol* 2017; **3**; 1051–1058.
21. McLaughlin J, Han G, Schalper KA *et al.* Quantitative assessment of the heterogeneity of PD-L1 expression in non-small-cell lung cancer. *JAMA Oncol.* 2016; **2**; 46–54.
22. Gainor JF. Moving programmed death-1 inhibitors to the front lines in non-small-cell lung cancer. *J. Clin. Oncol.* 2016; **34**; 2953–2955.
23. Kerr KM, Tsao MS, Nicholson AG *et al.* Programmed death-ligand 1 immunohistochemistry in lung cancer: in what state is this art? *J. Thorac. Oncol.* 2015; **10**; 985–989.
24. Borczuk AC, Allen TC. PD-L1 and lung cancer: the era of precision-ish medicine? *Arch. Pathol. Lab. Med.* 2016; **140**; 351–354.
25. Kerr KM, Hirsch FR. Programmed death ligand-1 immunohistochemistry: friend or foe? *Arch. Pathol. Lab. Med.* 2016; **140**; 326–331.
26. Kerr KM, Nicolson MC. Non-small cell lung cancer, PD-L1, and the pathologist. *Arch. Pathol. Lab. Med.* 2016; **140**; 249–254.
27. Sholl LM, Aisner DL, Allen TC *et al.* Programmed death ligand-1 immunohistochemistry – a new challenge for pathologists: a perspective from members of the Pulmonary Pathology Society. *Arch. Pathol. Lab. Med.* 2016; **140**; 341–344.
28. Cree IA, Booton R, Cane P *et al.* PD-L1 testing for lung cancer in the UK: recognizing the challenges for implementation. *Histopathology* 2016; **69**; 177–186.
29. Ratcliffe MJ, Sharpe A, Midha A *et al.* Agreement between programmed cell death ligand-1 diagnostic assays across multiple protein expression cut-offs in non-small cell lung cancer. *Clin. Cancer Res.* 2017; **23**; 3585–3591.
30. Gaule P, Smithy JW, Toki M *et al.* A quantitative comparison of antibodies to programmed cell death 1 ligand 1. *JAMA Oncol.* 2017; **3**; 256–259.
31. Neuman T, London M, Kania-Almog J *et al.* A harmonization study for the use of 22C3 PD-L1 immunohistochemical staining on Ventana's platform. *J. Thorac. Oncol.* 2016; **11**; 1863–1868.
32. Smith J, Robida MD, Acosta K *et al.* Quantitative and qualitative characterization of two PD-L1 clones: SP263 and E1L3N. *Diagn. Pathol.* 2016; **11**; 44.
33. Scheel AH, Dietel M, Heukamp LC *et al.* Harmonized PD-L1 immunohistochemistry for pulmonary squamous-cell and adenocarcinomas. *Mod. Pathol.* 2016; **29**; 1165–1172.
34. Abdel-Rahman O. Correlation between PD-L1 expression and outcome of NSCLC patients treated with anti-PD-1/PD-L1 agents: a meta-analysis. *Crit. Rev. Oncol. Hematol.* 2016; **101**; 75–85.
35. Hellmann MD, Rizvi NA, Goldman JW *et al.* Nivolumab plus ipilimumab as first-line treatment for advanced non-small-cell lung cancer (CheckMate 012): results of an open-label, phase 1, multicohort study. *Lancet Oncol.* 2017; **18**; 31–41.
36. Gniadek TJ, Li QK, Tully E, Chatterjee S, Nimmagadda S, Gabrielson E. Heterogeneous expression of PD-L1 in pulmonary squamous cell carcinoma and adenocarcinoma: implications for assessment by small biopsy. *Mod. Pathol.* 2017; **30**; 530–538.
37. Ilie M, Long-Mira E, Bence C *et al.* Comparative study of the PD-L1 status between surgically resected specimens and matched biopsies of NSCLC patients reveal major discordances: a potential issue for anti-PD-L1 therapeutic strategies. *Ann. Oncol.* 2016; **27**; 147–153.
38. Dietel M, Bubendorf L, Dingemans AM *et al.* Diagnostic procedures for non-small-cell lung cancer (NSCLC): recommendations of the European Expert Group. *Thorax* 2016; **71**; 177–184.
39. Zeng DQ, Yu YF, Ou QY *et al.* Prognostic and predictive value of tumor-infiltrating lymphocytes for clinical therapeutic research in patients with non-small cell lung cancer. *Oncotarget* 2016; **7**; 13765–13781.
40. Brambilla E, Le Teuff G, Marguet S *et al.* Prognostic effect of tumor lymphocytic infiltration in resectable non-small-cell lung cancer. *J. Clin. Oncol.* 2016; **34**; 1223–1230.
41. Bremnes RM, Busund LT, Kilvær TL *et al.* The role of tumor-infiltrating lymphocytes in development, progression, and prognosis of non-small cell lung cancer. *J. Thorac. Oncol.* 2016; **11**; 789–800.
42. Donnem T, Kilvaer TK, Andersen S *et al.* Strategies for clinical implementation of TNM-immunoscore in resected nonsmall-cell lung cancer. *Ann. Oncol.* 2016; **27**; 225–232.
43. Tokito T, Azuma K, Kawahara A *et al.* Predictive relevance of PD-L1 expression combined with CD8 + TIL density in stage III non-small cell lung cancer patients receiving concurrent chemoradiotherapy. *Eur. J. Cancer* 2016; **55**; 7–14.
44. Usó M, Jantus-Lewintre E, Bremnes RM *et al.* Analysis of the immune microenvironment in resected non-small cell lung cancer: the prognostic value of different T lymphocyte markers. *Oncotarget* 2016; **7**; 52849–52861.
45. Kadota K, Nitadori J, Ujiie H *et al.* Prognostic impact of immune microenvironment in lung squamous cell carcinoma: tumor-infiltrating CD10+ neutrophil/CD20+ lymphocyte ratio as an independent prognostic factor. *J. Thorac. Oncol.* 2015; **10**; 1301–1310.
46. Feng W, Li Y, Shen L, *et al.* Prognostic value of tumor-infiltrating lymphocytes for patients with completely resected stage IIIA (N2) non-small cell lung cancer. *Oncotarget* 2016; **7**; 7227–7240.
47. Yang CY, Lin MW, Chang YL, Wu CT, Yang PC. Programmed cell death-ligand 1 expression is associated with a favourable immune microenvironment and better overall survival in stage I pulmonary squamous cell carcinoma. *Eur. J. Cancer* 2016; **57**; 91–103.
48. Velcheti V, Schalper KA, Carvajal DE *et al.* Programmed death ligand-1 expression in non-small cell lung cancer. *Lab. Invest.* 2014; **94**; 107–116.
49. Uruga H, Bozkurtlar E, Huynh TG *et al.* Programmed cell death ligand (PD-L1) expression in stage II and III lung adenocarcinomas and nodal metastases. *J. Thorac. Oncol.* 2016; **12**; 458–466.

50. Kim MY, Koh J, Kim S, Go H, Jeon YK, Chung DH. Clinicopathological analysis of PD-L1 and PD-L2 expression in pulmonary squamous cell carcinoma: comparison with tumor-infiltrating T cells and the status of oncogenic drivers. *Lung Cancer* 2015; **88**; 24–33.
51. Huynh TG, Morales-Oyarvide V, Campo MJ *et al.* Programmed cell death ligand 1 expression in resected lung adenocarcinomas: association with immune microenvironment. *J. Thorac. Oncol.* 2016; **11**; 1869–1878.
52. Calles A, Liao X, Sholl LM *et al.* Expression of PD-1 and its ligands, PD-L1 and PD-L2, in smokers and never smokers with KRAS-mutant lung cancer. *J. Thorac. Oncol.* 2015; **10**; 1726–1735.
53. Ruffini E, Asioli S, Filosso PL *et al.* Clinical significance of tumor-infiltrating lymphocytes in lung neoplasms. *Ann. Thorac. Surg.* 2009; **87**; 365–371.
54. Schalper KA, Brown J, Carvajal-Hausdorf D *et al.* Objective measurement and clinical significance of TILs in non-small cell lung cancer. *J. Natl Cancer Inst.* 2015; **107**; dju435.
55. Koh J, Go H, Keam B *et al.* Clinicopathologic analysis of programmed cell death-1 and programmed cell death-ligand 1 and 2 expressions in pulmonary adenocarcinoma: comparison with histology and driver oncogenic alteration status. *Mod. Pathol.* 2015; **28**; 1154–1166.
56. Parra ER, Behrens C, Rodriguez-Canales J *et al.* Image analysis-based assessment of PD-L1 and tumor-associated immune cells density supports distinct intratumoral microenvironment groups in non-small cell lung carcinoma patients. *Clin. Cancer Res.* 2016; **22**; 6278–6289.
57. Schmidt LH, Kümmel A, Görlich D *et al.* PD-1 and PD-L1 expression in NSCLC indicate a favorable prognosis in defined subgroups. *PLoS ONE* 2015; **10**; e0136023.
58. Cooper WA, Tran T, Vilain R *et al.* PD-L1 expression is a favorable prognostic factor in early stage non-small cell carcinoma. *Lung Cancer* 2015; **89**; 181–188.
59. Shimoji M, Shimizu S, Sato K *et al.* Clinical and pathologic features of lung cancer expressing programmed cell death ligand 1 (PD-L1). *Lung Cancer* 2016; **98**; 69–75.
60. Tao D, Han X, Zhang N *et al.* Genetic alteration profiling of patients with resected squamous cell lung carcinomas. *Oncotarget* 2016; **7**; 36590–36601.
61. Paulsen EE, Kilvaer TK, Khanehkenari MR *et al.* Assessing PDL-1 and PD-1 in non-small cell lung cancer: a novel immunoscore approach. *Clin. Lung Cancer* 2016; **18**; 220–233.
62. Shukuya T, Mori K, Amann JM *et al.* Relationship between overall survival and response or progression-free survival in advanced non-small cell lung cancer patients treated with anti-PD-1/PD-L1 antibodies. *J. Thorac. Oncol.* 2016; **11**; 1927–1939.
63. Yu H, Boyle TA, Zhou C, Rimm DL, Hirsch FR. PD-L1 expression in lung cancer. *J. Thorac. Oncol.* 2016; **11**; 964–975.
64. Sun JM, Zhou W, Choi YL *et al.* Prognostic significance of PD-L1 in patients with non-small cell lung cancer: a large cohort study of surgically resected cases. *J. Thorac. Oncol.* 2016; **11**; 1003–1011.
65. National Comprehensive Cancer Network, Inc. Available at: https://www.nccn.org/store/login/login.aspx?ReturnURL=https://www.nccn.org/professionals/physician_gls/pdf/nscl.pdf (accessed 19 February 2017).
66. CAP/IASLC/AMP molecular testing guideline. Available at: https://www.iaslc.org/sites/default/files/wysiwyg-assets/5-20160616capiaslcamplungguideline-2016draftrecommendations_ocpfinal.pdf (accessed 19 February 2017).
67. Karasaki T, Nagayama K, Kawashima M *et al.* Identification of individual cancer-specific somatic mutations for neoantigen-based immunotherapy of lung cancer. *J. Thorac. Oncol.* 2016; **11**; 324–333.
68. Rooney MS, Shukla SA, Wu CJ, Getz G, Hacohen N. Molecular and genetic properties of tumors associated with local immune cytolytic activity. *Cell* 2015; **160**; 48–61.
69. Davoli T, Uno H, Wooten EC, Elledge SJ. Tumor aneuploidy correlates with markers of immune evasion and with reduced response to immunotherapy. *Science* 2017; **355**; eaaf8399.
70. Dong ZY, Zhong W, Zhang XC *et al.* Potential predictive value of TP53 and KRAS mutation status for response to PD-1 blockade immunotherapy in lung adenocarcinoma. *Clin. Cancer. Res.* 2017; **23**; 3012–3024.
71. Angulo B, Suarez-Gauthier A, Lopez-Rios F *et al.* Expression signatures in lung cancer reveal a profile for EGFR-mutant tumours and identify selective PIK3CA overexpression by gene amplification. *J. Pathol.* 2008; **214**; 347–356.
72. Socinski MA, Obasaju C, Gandara D *et al.* Clinicopathologic features of advanced squamous NSCLC. *J. Thorac. Oncol.* 2016; **11**; 1411–1422.
73. Choi M, Kadara H, Zhang J *et al.* Mutation profiles in early-stage lung squamous cell carcinoma with clinical follow-up and correlation with markers of immune function. *Ann. Oncol.* 2017; **28**; 83–89.
74. Cancer Genome Atlas Research Network. Comprehensive genomic characterization of squamous cell lung cancers. *Nature* 2012; **489**; 519–525.
75. Lee HY, Lee SH, Won JK *et al.* Analysis of fifty hotspot mutations of lung squamous cell carcinoma in never-smokers. *J. Korean Med. Sci.* 2017; **32**; 415–420.
76. Cha YJ, Kim HR, Lee CY, Cho BC, Shim HS. Clinicopathological and prognostic significance of programmed cell death ligand-1 expression in lung adenocarcinoma and its relationship with p53 status. *Lung Cancer* 2016; **97**; 73–80.
77. Casey SC, Tong L, Li Y *et al.* MYC regulates the antitumor immune response through CD47 and PD-L1. *Science* 2016; **352**; 227–231.
78. Guo Q, Sun Y, Yu S *et al.* Programmed cell death-ligand 1 (PD-L1) expression and fibroblast growth factor receptor 1 (FGFR1) amplification in stage III/IV lung squamous cell carcinoma (SQC). *Thorac. Cancer* 2017; **8**; 73–79.
79. Xu C, Fillmore CM, Koyama S *et al.* Loss of Lkb1 and Pten leads to lung squamous cell carcinoma with elevated PD-L1 expression. *Cancer Cell* 2014; **25**; 590–604.
80. Sharma P, Allison JP. Immune checkpoint targeting in cancer therapy: toward combination strategies with curative potential. *Cell* 2015; **161**; 205–214.

Supporting Information

Additional Supporting Information may be found in the online version of this article:

Table S1. *TP53* PCR primer sequences

Table S2. Genes included in the Oncomine™ Focus Assay panel